JOURNAL OF SOLID STATE CHEMISTRY 72, 24–30 (1988)

Ferromagnetic $R_2Mn_2O_7$ Pyrochlores (R = Dy–Lu, Y)*

M. A. SUBRAMANIAN, C. C. TORARDI, D. C. JOHNSON,**
J. PANNETIER,† AND A. W. SLEIGHT

E. I. du Pont de Nemours and Company, Central Research and Development Department,‡ Experimental Station, Wilmington, Delaware 19898

Received February 3, 1987

Pyrochlores of the type $R_2Mn_2O_7$ have been prepared and characterized where R is Dy, Ho, Er, Tm, Yb, Lu, or Y. All are semiconductors with activation energies ranging from 0.37 to 0.51 eV, which correlate very well with the electronegativity of R. Structural refinements on $Er_2Mn_2O_7$ and $Y_2Mn_2O_7$ confirm the pyrochlore structure and the stoichiometry. Highly anisotropic thermal motion is found for the rare-earth cation, consistent with its very unusual environment. These $R_2Mn_2O_7$ pyrochlores all possess magnetic ordering temperatures in the range 20 to 40 K. The susceptibility data above T_c indicate dominant ferromagnetic interactions, i.e., positive Weiss constants. The field dependence data below T_c are also suggestive of ferromagnetism. Nonetheless, the magnetic behavior is complex, and there may be no spontaneous moments in the absence of an applied field.

Introduction

A large number of complex oxides with the formula $A_2M_2O_7$ crystallize with pyrochlore-type structure ($Fd3m$, Z = 8) where A is a 2+ or 3+ ion and M is a 5+ or 4+ ion, respectively (*1, 2*). In the pyrochlore structure, A cations are coordinated to eight oxygen ions whereas M cations are coordinated to six oxygen ions in a nearly octahedral environment. Many of the pyrochlores known are of the type $A_2^{3+}M_2^{4+}O_7$. This is due to the fact that a large number of A^{3+} and M^{4+} cations have suitable ionic radii for the formation of the pyrochlore structure. High-pressure techniques have been used to stabilize the pyrochlore structure when the radius of M^{4+} falls below 0.58 Å (*3–5*).

Brisse (*6*) attempted to synthesize a $Yb_2Mn_2O_7$ pyrochlore phase by reacting MnO_2 and Yb_2O_3 at 1500 psi oxygen pressure but was not successful. Fujinaka *et al.* (*5*) reported the formation of $Y_2Mn_2O_7$ and $Tl_2Mn_2O_7$ pyrochlores at 1000°C under 40 to 60 kbar pressure. In this paper, we report the synthesis and characterization of $R_2Mn_2O_7$ compounds obtained under hydrothermal conditions. Single crystals of $Y_2Mn_2O_7$ and $Er_2Mn_2O_7$ were grown, and their structures were refined. Magnetic and electrical properties are also reported.

* Dedicated to John B. Goodenough.

** Current address: Department of Chemistry, University of Oregon, Eugene, OR 97403.

† Current address: Institut Max Von Laue-Paul Langevin, 156X, 38042 Grenoble Cedex, France.

‡ Contribution No. 4218.

0022-4596/88 $3.00

Experimental

Synthesis

The rare-earth oxides were all of at least 99.9% purity; $NaClO_3$ and NaOH were reagent grade. MnO_2 was puratronic grade from Johnson & Matthey.

Two or three grams of MnO_2 and R_2O_3 in a 2:1 molar ratio were first mixed thoroughly for a half-hour in an agate mortar and loaded into a gold tube ($\frac{3}{8}$-in. dia × 5-in. length). Then, 0.2 g each of $NaClO_3$ and NaOH were added to the tube along with 3 ml of H_2O. The tube was sealed and heated to 500°C for 10 hr under 3 kbar pressure and cooled to room temperature at the rate of 10°C/hr. The resulting solid was washed with water to remove NaCl and any unreacted $NaClO_3$. Crystals suitable for single crystal X-ray diffraction studies were grown by using $KMnO_4$ and R_2O_3 as starting materials.

X-Ray Powder Diffraction

Powder X-ray diffraction data were obtained with a Guinier–Hägg type focusing camera using Cu$K_{\alpha 1}$ radiation and Si (a = 5.4305 Å) as an internal standard. Cell dimensions were refined by least squares and are given in Table I.

TABLE I

CELL DIMENSIONS, DENSITIES, AND ELECTRICAL DATA FOR $A_2Mn_2O_7$ COMPOUNDS

Compound	a_0 (Å)	Density (g/ml) Obs.	Calc.	ρ (ohm-cm) 300 K	E_a (eV)
$Dy_2Mn_2O_7$	9.929	7.3	7.42	1×10^6	0.37
$Ho_2Mn_2O_7$	9.905	7.5	7.54	8×10^7	0.45
$Er_2Mn_2O_7$	9.869	7.6	7.68	3×10^7	0.47
$Tm_2Mn_2O_7$	9.847	—	7.78	2×10^7	0.48
$Yb_2Mn_2O_7$	9.830	7.9	7.94	—	—
$Lu_2Mn_2O_7$	9.815	—	8.03	2×10^8	0.51
$Y_2Mn_2O_7$	9.901	5.4	5.47	3×10^6	0.38
$Tl_2Mn_2O_7$[a]	9.890	8.6	8.66	$\sim 1 \times 10$	0.09

[a] Data for $Tl_2Mn_2O_7$ are taken from Ref. (5) for comparison.

TABLE II

SUMMARY OF CRYSTAL DATA, COLLECTION DATA, AND REFINEMENT OF STRUCTURES FOR $Er_2Mn_2O_7$ AND $Y_2Mn_2O_7$

	$Er_2Mn_2O_7$	$Y_2Mn_2O_7$
Dimensions (mm)	0.08 × 0.13 × 0.13	0.10 × 0.14 × 0.14
Cell constant, a (Å)	9.875(4)	9.902(1)
μ (cm^{-1})	399.0	287.0
Total reflections	1616	1661
Independent reflections	64	48
Data/parameters	8.1	6
Extinction factor (mm)	0.15×10^{-4}	0.35×10^{-4}
R	0.017	0.025
R_w	0.021	0.027

Crystal Structure Refinements

Experimental information for single crystal X-ray data collection and structural refinement is given in Table II for the Er and Y manganese pyrochlores. The data were collected in a θ-2θ scan mode from 4 ≤ θ ≤ 30° on an Enraf Nonius CAD4 diffractometer using MoK_α radiation and a graphite monochromator. The data were treated for Lorentz and polarization effects, and a correction for absorption was applied using DIFABS (7) for $Er_2Mn_2O_7$ and an empirical method for $Y_2Mn_2O_7$. Rare-earth cations were refined using anisotropic thermal parameters. Table III lists the atomic positional and thermal param-

TABLE III

POSITIONAL AND THERMAL PARAMETERS FOR THE ATOMS OF $Er_2Mn_2O_7$ AND $Y_2Mn_2O_7$

Atom	Site	x	y	z	B^a (Å^2)
Er	16*d*	0.50	0.50	0.50	0.3(1)
Mn	16*c*	0.00	0.00	0.00	0.1(0)
O1	8*b*	0.3750	0.3750	0.3750	0.3(3)
O2	48*f*	0.3281(8)	0.1250	0.1250	0.5(1)
Y	16*d*	0.50	0.50	0.50	0.3(1)
Mn	16*c*	0.00	0.00	0.00	0.1(1)
O1	8*b*	0.3750	0.3750	0.3750	0.1(3)
O2	48*f*	0.3274(8)	0.1250	0.1250	0.2(1)

[a] The final anisotropic thermal parameters for the rare-earth atoms are $U_{11} = U_{22} = U_{33} = 0.0033(3)$(Er), 0.0033(7)(Y), and $U_{12} = U_{13} = U_{23} = -0.0013(2)$(Er), −0.0015(5)(Y).

TABLE IV

IMPORTANT INTERATOMIC DISTANCES (Å) AND ANGLES (DEG) FOR $Er_2Mn_2O_7$ AND $Y_2Mn_2O_7$

		$Er_2Mn_2O_7$		
Er –O1	2.1380(5)	(2×)	O2 –Mn –O2	96.0(3)
Er –O2	2.435(6)	(6×)	O2 –Mn –O2	84.0(3)
Mn –O2	1.908(3)	(6×)	Mn –O2 –Mn	132.3(4)
Mn –Mn	3.491(1)			
		$Y_2Mn_2O_7$		
Y –O1	2.1439(1)	(2×)	O2 –Mn –O2	95.7(3)
Y –O2	2.447(6)	(6×)	O2 –Mn –O2	84.3(3)
Mn –O2	1.911(3)	(6×)	Mn –O2 –Mn	132.7(5)
Mn –Mn	3.5009(3)			

eters for both compounds, and important interatomic distances and angles are given in Table IV.

Electrical Measurements

Electrical conductivity measurements were performed on samples in the form of very dense pellets (formed at 600°C and 58 kbar pressure) using a Keithly 617 electrometer and sputtered gold electrodes in the temperature range 300 to 600 K.

Magnetic Measurements

The magnetic susceptibility data were collected over the range 1.8–325 K using a Faraday balance. Samples were suspended on a 1-mm quartz rod from the arm of a Cahn 2000 electrobalance. The sample container (4.2 × 10 mm) was fashioned from high-purity Spectrosil quartz. An electromagnet (Walker Scientific) supplied variable fields up to 22.5 kG. The magnetic field gradient was calibrated using $HgCo(SCN)_4$ as a standard and varied by less than 1% in the area of the sample container. Temperature was controlled with a digital temperature controller (Oxford Instruments 3120) using a Au/Fe versus chromel/P thermocouple. A calibrated silicon diode resistance thermometer was used to measure the sample temperature, independently of the controlling thermocouple, over the entire temperature range. The Cahn balance was operated on the 100-mg scale, on which a sensitivity under ideal conditions of 0.001 mg can be achieved. Under normal operating conditions, the sensitivity is the larger of 0.02 mg or 0.1% of the force being measured. A typical error estimate in the measurement of the susceptibilities reported in this paper is 0.5%. The susceptibilities have been corrected for the intrinsic diamagnetism of the sample container and the diamagnetism of the electronic cores of the constituent atoms.

Results

Synthesis

Single-phase $R_2Mn_2O_7$ compounds were obtained for R = Dy–Lu and Y under the preparative conditions employed (3 kbar). The compounds were black in color and generally formed as small, octahedral crystals. Powder X-ray diffraction patterns of all the compounds could be indexed as face-centered cubic cells; cell edges and densities are given in Table I. A plot of the radius of R^{3+} (*8*) and unit cell parameter showed linear behavior as expected (Fig. 1).

All the pyrochlore products prepared with $NaClO_3$ were analyzed for Na and Cl, and none of them showed the presence of these elements above the detection limits of the analysis.

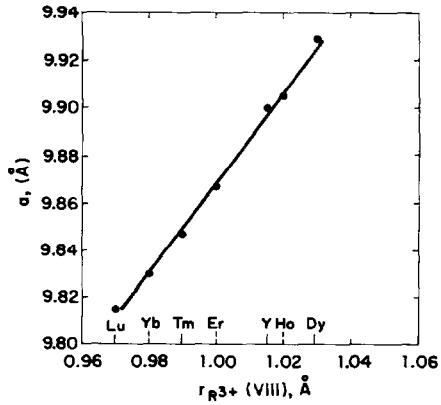

FIG. 1. Cell edge of $R_2Mn_2O_7$ vs radius of R^{3+}.

Structure

The pyrochlore structure of composition $R_2Mn_2O_7$ is built of MnO_6 octahedra with each corner of the octahedron being shared with another MnO_6 unit. However, instead of forming linear chains, as in the perovskite structure, the octahedra are linked in a zig-zag pattern along the chains in the ⟨110⟩ directions with a Mn–O–Mn bond angle of 132.5°. These Mn–O chains connect to the RO_8 polyhedra by the sharing of edges.

In the MnO_6 octahedron (Fig. 2a), all six Mn–O bonds are equivalent. The Mn–O bond lengths for $Y_2Mn_2O_7$ and $Er_2Mn_2O_7$ are essentially identical, 1.910 Å. This length compares very well with the sum of ionic radii (*8*) for six-coordinate Mn^{4+} and four-coordinate O^{2-}, 1.91 Å. The site symmetry of the MnO_6 "octahedron" is actually $\bar{3}m$ (D_{3d}); thus, the octahedron distorts so that O–Mn–O bond angles of 96 and 84° are observed. Figure 2b shows the atomic arrangement of an ErO_8 polyhedron. Two O1 atoms cap opposite triangular faces of a flattened trigonal antiprism of O2 atoms. The site symmetry is $\bar{3}m$ (D_{3d}). The *R* atom lies on a threefold axis, and its thermal ellipsoid is an ellipsoid of rotation where the unique axis is the threefold axis. Therefore, the ellipsoid may be elongated or compressed along this axis. Thermal ellipsoids for both the Er and Y compounds were found to be very compressed along the threefold axis. The rms displacement is ~0.02 Å along the axis, and ~0.07 Å perpendicular to the axis. This mode of vibration is physically reasonable because there are two very short *R*–O bonds along the threefold axis that restrict thermal motion in this direction. Similar behavior has been previously noted for the pyrochlore structure (*9*).

Each RO_8 unit is linked to six other RO_8 units by the sharing of oxygen atoms O1. These oxygen atoms are bonded to four *R* atoms and possess $\bar{4}3m$ (T_d) symmetry. Oxygen atoms O2 are "tetrahedrally" bonded to two *R* and two Mn atoms, but their site symmetry is actually *mm* (C_{2v}).

Thermal Stability

In order to test the thermal stability of $R_2Mn_2O_7$ pyrochlores, all of them were heated in air to various temperatures in a thermogravimetric balance. All the pyrochlores were stable up to 800°C, and the weight loss corresponds to loss of one oxygen atom. X-ray powder diffraction patterns of the $R_2Mn_2O_7$ compounds obtained

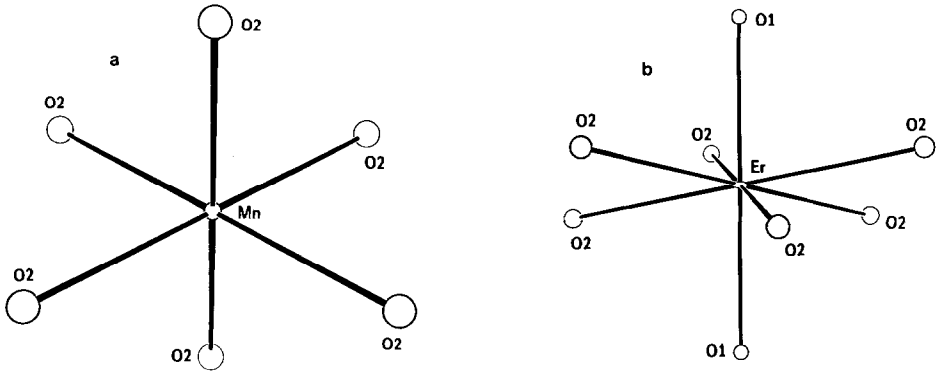

FIG. 2. (a) An ORTEP drawing of an MnO_6 octahedron in $Er_2Mn_2O_7$. (b) An ErO_8 polyhedron showing the anisotropic thermal ellipsoid of Er compressed along the threefold axis which includes the O1 atoms.

after heating at 900°C in air showed the presence of only $LnMnO_3$ perovskites.

Electrical Properties

Electrical measurements indicate that all $R_2Mn_2O_7$ pyrochlores are semiconducting. The activation energies and the room temperature resistivities are given in Table I.

Magnetic Properties

All the $R_2Mn_2O_7$ pyrochlores exhibit ferromagnetic behavior with Curie temperatures of 20 to 40 K. The results are summarized in Table V and Figs. 3 and 4.

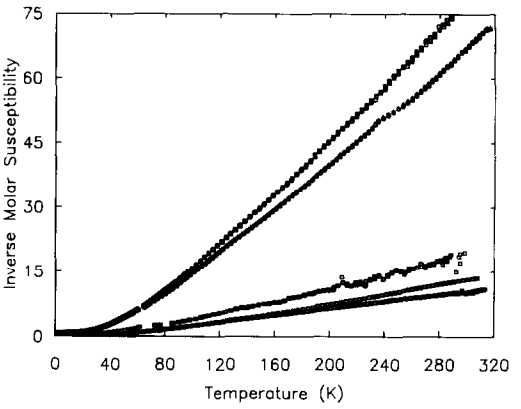

FIG. 3. Inverse magnetic susceptibility vs temperature for $R_2Mn_2O_7$ pyrochlores, R = Lu, Y, Tm, Er, and Ho (top to bottom).

Discussion

Despite the widespread occurrence of the pyrochlore structure, the magnetic properties of compounds with this structure have not been extensively investigated. The magnetic interactions in the pyrochlore structure are very interesting due to the arrangement of the cations. The M cations can be viewed as clustered into tetrahedral units which share corners to form infinite, intersecting chains. This cation arrangement makes it impossible for the nearest-neighbor spins to be aligned antiparallel to one another throughout the chains. The antiferromagnetic interaction between any two adjacent cations is frustrated by the presence of the other cations making up the tetrahedron. This magnetic frustration results in spin glass or ferromagnetic behavior in some pyrochlore compounds (*10*).

Studies of ferromagnetic $R_2Mo_2O_7$ pyrochlores have suggested that the ferromagnetism in these phases is directly related to their metallic behavior (*11*). The proposed magnetic coupling is through the conduction mechanism, the conduction

TABLE V

SUMMARY OF MAGNETIC PROPERTIES

	μ_R	μ_{calc}[a]	μ_{obs}	θ (K)	T_c (K)
$Y_2Mn_2O_7$	0	5.4	5.4	50 ± 10	20 ± 5
$Lu_2Mn_2O_7$	0	5.4	4.9	70 ± 10	23 ± 5
$Yb_2Mn_2O_7$	4.5	8.3	7.6	41 ± 3	35 ± 5
$Tm_2Mn_2O_7$	7.6	12.0	10.4	56 ± 8	30 ± 5
$Er_2Mn_2O_7$	9.6	14.6	13.3	40 ± 5	35 ± 5
$Ho_2Mn_2O_7$	10.6	15.9	14.4	33 ± 5	37 ± 5
$Dy_2Mn_2O_7$	10.6	15.9	14.4	43 ± 2	40 ± 5
$Tl_2Mn_2O_7$[b]	0	5.4	5.0	167 ± 2	117

[a] $\mu_{calc} = \sqrt{2\mu_R^2 + 2\mu_{Mn}^2}$, where $\mu_{Mn} = 3.8$.

[b] Data for $Tl_2Mn_2O_7$ are taken from Ref. (*5*) except for θ which was determined in this study.

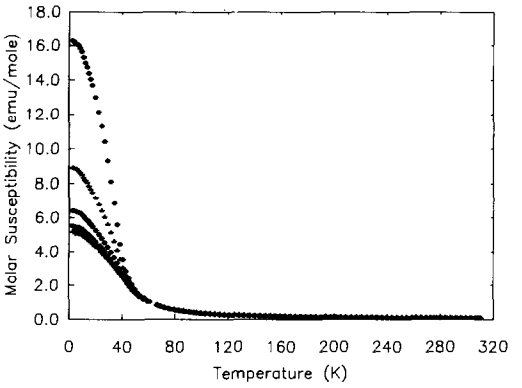

FIG. 4. Field dependence of molar susceptibility for $Er_2Mn_2O_7$, H_0 = 5.3, 11.4, 15.9, 18.4, 19.5 kG (top to bottom).

band being formed of delocalized Mo 4*d* electrons. The magnetic ordering temperature was found to increase with an increase in conductivity as expected for this coupling mechanism. The existence of ferromagnetic behavior in the $R_2Mn_2O_7$ and $R_2V_2O_7$ (*12–15*) pyrochlores which are semiconducting indicates that metallic behavior is not a necessary condition for ferromagnetism. Neutron diffraction studies are underway to elucidate the magnetic structure of $Y_2Mn_2O_7$.

The ferromagnetic behavior of the $R_2Mn_2O_7$ pyrochlores appears to result from the Mn cation arrangement. For a Mn–O–Mn angle of 180°, superexchange interactions between the cations are completely antiferromagnetic in nature (*16*). However, there are both ferromagnetic and antiferromagnetic superexchange interactions for a Mn–O–Mn angle of 90° (*17*). In the pyrochlore structure, the Mn–O–Mn angle is ~130°. Since antiferromagnetic interactions are generally stronger than ferromagnetic interactions, one would expect the Mn^{4+}–O–Mn^{4+} superexchange interactions in the pyrochlore structure to be antiferromagnetic in nature. However, the weaker ferromagnetic interactions are observed to dominate, at least in the presence of an applied field, in the $R_2Mn_2O_7$ pyrochlores because of the frustration of the antiferromagnetic interaction due to the tetrahedral arrangement of the Mn^{4+} cations. We conclude that there are two essential features responsible for the ferromagnetism in the pyrochlore structure: (1) the tetrahedral arrangement of the *M* cations and (2) the strong deviation from linearity in the *M*–O–*M* bonds.

The Curie temperatures of the $R_2Mn_2O_7$ pyrochlores varied between 20 and 40 K and are given in Table V. No correlations were found relating the Curie temperature with rare-earth cation radius, rare-earth moment, or Mn–O–Mn bond angles. The Curie temperature for the thallium compound was in agreement with that previously published (*5*). The observed moments for the $R_2Mn_2O_7$ pyrochlores basically agree with the moment calculated assuming no magnetic interactions between Mn and rare-earth cations above the Curie temperature as shown in Table V.

The electrical properties (Table I) show a trend toward lower activation energies with increasing size of the *R* cation. It is likely that the activation energies represent the activation energy of electron hopping from site to site within the 3*d* band of Mn. The same trend has been observed for $R_2M_2O_7$ pyrochlores where *M* is Mo, Ru, or Ir. Since *M*–O distances do not change significantly within a particular *M* series, the explanation could lie in the *M*–O–*M* angle which increases regularly (131.2 to 133.5°) with increasing size of the *R* cation. However, this angle change may be too small to be significant, and the activation energy for $Y_2Mn_2O_7$ does not follow this trend. However, a plot of E_a vs Pauling's electronegativities (Fig. 5) shows a smooth curve. This strongly suggests an inductive effect. As the *A* cation becomes more electropositive, the Mn–O bonding becomes stronger, and the mobility of the 3*d* electrons increases. Such effects are well documented. For example, the charge transfer band in

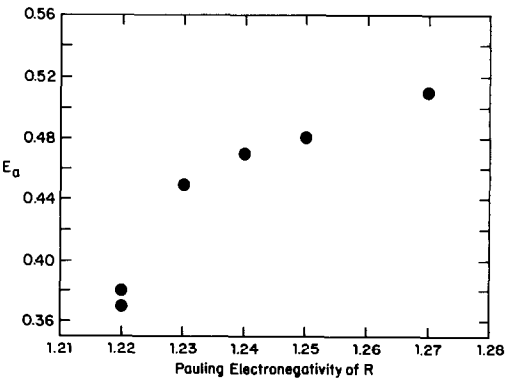

FIG. 5. Activation energy from electrical resistivity data vs the Pauling electronegativity value of *R* in the $R_2Mn_2O_7$ series.

$AMoO_4$ and AWO_4 compounds moves to higher energies with increasing electropositive character of A, indicating that the Mo–O or W–O bonding has become stronger (*18*). An analogous inductive effect of A cations in perovskite series like $ACrO_3$ and $AFeO_3$ has been previously described by Goodenough and Longo (*19*).

The electrical properties of $Tl_2Mn_2O_7$ are not explained by the arguments of the preceding paragraph. Since Tl is less electropositive than the rare earths, a higher activation energy for $Tl_2Mn_2O_7$ would be predicted. However, the 6*s* band of Tl lies close in energy to the 3*d* levels so that mixing is anticipated. This mixing broadens the 3*d* band and increases the mobility of the 3*d* electrons and increases the magnetic ordering temperature.

References

1. M. A. SUBRAMANIAN, G. ARAVAMUDAN, AND G. V. SUBBA RAO, *Prog. Solid State Chem.* **15,** 55 (1983).
2. A. W. SLEIGHT, *Mater. Res. Bull.* **9,** 1177 (1974).
3. R. D. SHANNON AND A. W. SLEIGHT, *Inorg. Chem.* **7,** 1649 (1968).
4. C. CHATEAU AND J. LORIERS, *Compt. Rend. (Paris) C* **288,** 421 (1979).
5. H. FUJINAKA, N. KINAMURA, M. KOIZUMI, Y. MIYAMOTO, AND S. KUME, *Mater. Res. Bull.* **14,** 1133 (1979).
6. F. BRISSE, Ph.D thesis, Dalhousie Univ., Halifax, Nova Scotia (1967).
7. N. WALKER AND D. STUART, *Acta Crystallogr. A* **39,** 158 (1983).
8. R. D. SHANNON AND C. T. PREWITT, *Acta Crystallogr. B* **25,** 925 (1969).
9. A. W. SLEIGHT, *Inorg. Chem.* **7,** 1704 (1968).
10. G. FEREY, M. LEBLANC, R. DE PAPE, AND J. PANNETIER, *in* "Inorganic Solid Fluorides" (P. Hagenmuller, Ed.), p. 395, Academic Press, New York (1985).
11. M. SATO, XU YAN, AND J. E. GREEDAN, *Z. Anorg. Allgem. Chem.* **540/541,** 177 (1986).
12. G. V. BAZREV, D. V. MAKAROVA, V. Z. OBOLDIN, AND G. P. SHVEIKIN, *Dokl. Akad. Nauk. SSSR* **230,** 869 (1976).
13. T. SHIN-IKE, G. ADACHI, AND J. SHIOKAWA, *Mater. Res. Bull.* **12,** 1149 (1977).
14. L. SODERHOLM AND J. E. GREEDAN, *Mater. Res. Bull.* **14,** 1449 (1979).
15. L. SODERHOLM, J. E. GREEDAN, AND M. F. COLLINS, *J. Solid State Chem.* **35,** 385 (1980).
16. J. B. GOODENOUGH, "Magnetism and the Chemical Bond," p. 170, Wiley, New York (1966).
17. J. B. GOODENOUGH, "Magnetism and the Chemical Bond," p. 181, Wiley, New York (1966).
18. F. A. KRÖGER, "Some Aspects of the Luminescence of Solids," Elsevier, New York (1948).
19. J. B. GOODENOUGH AND J. M. LONGO, *in* "Landolt–Börnstein, Group III"/Vol. 4a (K. Hellwege, Ed.), Vol. 4a, p. 257, Springer-Verlag, New York (1970).